Pharmaceutical Research, Vol. 24, No. 3, March 2007 (© 2007)
DOI: 10.1007/s11095-006-9176-1

Research Paper

Transport of Nicotinate and Structurally Related Compounds by Human SMCT1 (SLC5A8) and Its Relevance to Drug Transport in the Mammalian Intestinal Tract

Elangovan Gopal,[1] Seiji Miyauchi,[1] Pamela M. Martin,[1] Sudha Ananth,[1] Penny Roon,[2] Sylvia B. Smith,[2] and Vadivel Ganapathy[1,3]

Received July 31, 2006; accepted October 5, 2006; published online January 24, 2007

Purpose. To examine the involvement of human SMCT1, a Na^+-coupled transporter for short-chain fatty acids, in the transport of nicotinate/structural analogs and monocarboxylate drugs, and to analyze its expression in mouse intestinal tract.
Materials and Methods. We expressed human SMCT1 in *X. laevis* oocytes and monitored its function by [^{14}C]nicotinate uptake and substrate-induced inward currents. SMCT1 expression in mouse intestinal tract was examined by immunofluorescence.
Results. [^{14}C]Nicotinate uptake was several-fold higher in SMCT1-expressing oocytes than in water-injected oocytes. The uptake was inhibited by short-chain/medium-chain fatty acids and various structural analogs of nicotinate. Exposure of SMCT1-expressing oocytes to nicotinate induced Na^+-dependent inward currents. Measurements of nicotinate flux and associated charge transfer into oocytes suggest a Na^+:nicotinate stoichiometry of 2:1. Monocarboxylate drugs benzoate, salicylate, and 5-aminosalicylate are also transported by human SMCT1. The transporter is expressed in the small intestine as well as colon, and the expression is restricted to the lumen-facing apical membrane of intestinal and colonic epithelial cells.
Conclusions. Human SMCT1 transports not only nicotinate and its structural analogs but also various monocarboxylate drugs. The transporter is expressed on the luminal membrane of the epithelial cells lining the intestinal tract. SMCT1 may participate in the intestinal absorption of monocarboxylate drugs.

KEY WORDS: SMCT1; intestinal tract; monocarboxylate drugs; aminosalicylates; electrophysiology.

INTRODUCTION

Sodium-coupled monocarboxylate transporter 1 (SMCT1; SLC5A8) transports short-chain fatty acids in a Na^+-coupled and electrogenic manner (1–3). The transporter was originally identified as a putative tumor suppressor in the colon (4) and the ability of the transporter to transport butyrate, an inhibitor of histone deacetylases, may underlie its tumor-suppressive role (5,6). SMCT1 is expressed in the colon, small intestine, kidney, thyroid gland, and brain (5,6). In the intestinal tract, the physiologic function of the transporter is likely to be in the absorption of short-chain fatty acids generated in the lumen by bacterial fermentation of dietary fiber. In the kidney, the transporter plays an obligatory role in the reabsorption of lactate from the glomerular filtrate and conserves this metabolite for gluconeogenesis (3,7). Since β-hydroxybutyrate is also a substrate for the transporter, SMCT1 functions in the reabsorption of this ketone body in the kidney and in the neuronal uptake of this ketone body for subsequent use in energy production (8). The handling of β-hydroxybutyrate by SMCT1 becomes important under conditions such as prolonged starvation, pregnancy, and uncontrolled diabetes when this metabolite is generated in the liver and released into circulation as an energy source alternative to glucose to the brain (9,10). Even though a previous study demonstrated the ability of SMCT1 to transport iodide (11), subsequent studies showed that the transporter possesses little or no ability to transport iodide (1–3,12); therefore, the biologic role of this transporter in thyroid gland remains unknown. SMCT1 has thus far been cloned from human (1,4), mouse (3), and rat (unpublished data) tissues.

Mouse SMCT1 also functions as a vitamin transporter with ability to transport the B-complex vitamin nicotinate in a Na^+-coupled manner. (13) Human SMCT1 also is capable of nicotinate transport and its transport function is

[1] Departments of Biochemistry and Molecular Biology, Medical College of Georgia, Augusta, Georgia 30912, USA.
[2] Departments of Cellular Biology and Anatomy, Medical College of Georgia, Augusta, Georgia 30912, USA.
[3] To whom correspondence should be addressed. (e-mail: vganapat@mail.mcg.edu)

inhibitable by ibuprofen and other structurally related non-steroidal anti-inflammatory drugs (14). Here we examined the ability of human SMCT1 to transport various structural analogs of nicotinate. These studies showed that SMCT1 transports not only nicotinate but also a variety of monocarboxylate drugs such as benzoate, salicylate, and aminosalicylates. Immunofluorescence studies showed that the transporter is expressed in the apical membrane of the epithelial cells lining the intestine and colon, suggesting a potential role for this transporter in the absorption of monocarboxylate drugs in the mammalian intestinal tract.

MATERIALS AND METHODS

Materials

[^{3}H]Nicotinate (specific radioactivity, 55 mCi.mmol) was purchased from American Radiolabeled Chemicals (St. Louis, MO). Structural analogs of nicotinate and monocarboxylate drugs were obtained from Sigma (St. Louis, MO). Human SMCT1 was originally cloned from human intestine (1).

Functional Expression of Human SMCT1 in *X. laevis* Oocytes

Capped cRNA from human SMCT1 cDNA (cloned in pGH19, a *X. laevis* oocyte expression vector, kindly provided by Peter S. Aronson, Yale University) was synthesized using the mMESSAGE-mMACHINE kit (Ambion, Austin, TX). Mature oocytes from *X. laevis* were isolated by treatment with collagenase A (1.6 mg/ml), manually defolliculated and maintained at 18°C in modified Barth's medium, supplemented with 25 μg/ml gentamicin as described previously (1). On the following day, oocytes were injected with 50 ng of cRNA. Water-injected oocytes served as controls. The research adhered to the "Principles of Laboratory Animal Care" (NIH publication #85-23, revised in 1985) and was approved by the institutional Committee for Animal Use in Research and Education.

The oocytes were used for measurements of [^{3}H]nicotinate uptake and for electrophysiological studies 3–7 days after cRNA injection. Uptake of [^{3}H]nicotinate (unlabeled plus radiolabeled nicotinate, 100 or 200 μM) into water-injected and SMCT1-expressing oocytes was measured for 60 min with eight to ten oocytes for each measurement, as described previously (13). Electrophysiological studies were performed by the two-microelectrode voltage-clamp method. Oocytes were perifused with a NaCl-containing buffer (100 mM NaCl, 2 mM KCl, 1 mM $MgCl_2$, 1 mM $CaCl_2$, 10 mM Hepes, pH 7.5), followed by the same buffer containing nicotinate and its structural analogs. The membrane potential was clamped at −50 mV. The differences between the steady-state currents measured in the presence and absence of substrates were considered as the substrate-induced currents. In the analysis of the saturation kinetics of substrate-induced currents, the kinetic parameter $K_{0.5}$ (i.e., the substrate concentration necessary for the induction of half-maximal current) was calculated by fitting the values of the substrate-induced currents to the Michaelis–Menten equation. The Na^+-activation kinetics of substrate-induced currents was analyzed by measuring the substrate-specific currents in the presence of increasing concentrations of Na^+. The concentration of Na^+ was varied by adjusting the concentration of NaCl in the perifusion buffer appropriately with equimolar concentrations of *N*-methyl-D-glucamine chloride. The data for the Na^+-dependent currents were analyzed according to the Hill equation to determine the Hill coefficient (h, the number of Na^+ ions involved in the activation process) and $K_{0.5}$ for Na^+ (i.e., the concentration of Na^+ necessary for half-maximal activation). Since the expression levels varied significantly from oocyte to oocyte, kinetic analyses were done by normalizing the expression levels to eliminate the variations among different oocytes. This was done by taking the maximally induced SMCT1-specific currents in each kinetic experiment in individual oocytes as 1. To investigate the current–voltage (I–V) relationship, step changes in membrane potential were applied, each for a duration of 100 ms in 20-mV increments.

Determination of Substrate/Charge Transfer Ratio

The charge-to-substrate transfer ratio was determined for nicotinate in four different oocytes as described previously (1,3,15,16). The oocytes were perifused with 100 μM nicotinate (unlabeled nicotinate, 85 μM; radiolabeled nicotinate, 15 μM), and inward currents were monitored over a period of 8–10 min. At the end of the experiment, the amounts of nicotinate transported into the oocytes was calculated by measuring the radioactivity associated with the oocytes. The area within the curve describing the relationship between the time and inward current was integrated to calculate the charge transferred into the oocyte during incubation with nicotinate. The values for substrate transfer and charge transfer were used to determine the substrate/charge transfer ratio.

Data Analysis

Electrophysiologic measurements were made with four different oocytes for each experimental point and the data are presented as means ± S. E. The kinetic parameters were determined using the computer program Sigma Plot, version 6.0 (SPSS, Inc., Chicago, IL). This was done by fitting the data from substrate saturation kinetics to the Michaelis–Menten equation and those from Na^+-activation kinetics to the Hill equation. The charge/substrate transfer ratio was determined independently in four different oocytes.

Immunofluorescence Localization of SMCT1 in Mouse and Human Intestinal Tract

The generation of anti-SMCT1 antibody and its specificity have been described previously (8). The experimental procedure for immunofluorescence analysis followed our previously published protocol (8). Sections of different parts of the intestinal tract from adult mice were frozen in OCT embedding compound and 10 μm thick cryosections prepared. Cryosections were fixed in ice-cold acetone, blocked with 10% normal goat serum and incubated for 3 h at 25°C and overnight at 4°C with the primary antibody specific for SMCT1. After rinsing, sections were incubated overnight at

4°C with fluorophore (red)-conjugated secondary antibody (goat anti-rabbit IgG coupled to Alexa Flour 568). DAPI (blue fluorescence) was used as the nuclear stain. As negative controls, some sections were incubated with the primary antibody which had been neutralized with the antigenic peptide. Sections of human colon were processed similarly. Sections were examined using a Zeiss Axioplan 2 fluorescent microscope.

RESULTS

Transport of Nicotinate and Its Structural Analogs via Human SMCT1

Figure 1 lists the structural analogs of nicotinate and related monocarboxylate drugs that were used in the present study. Figure 2a shows that human SMCT1 is expressed

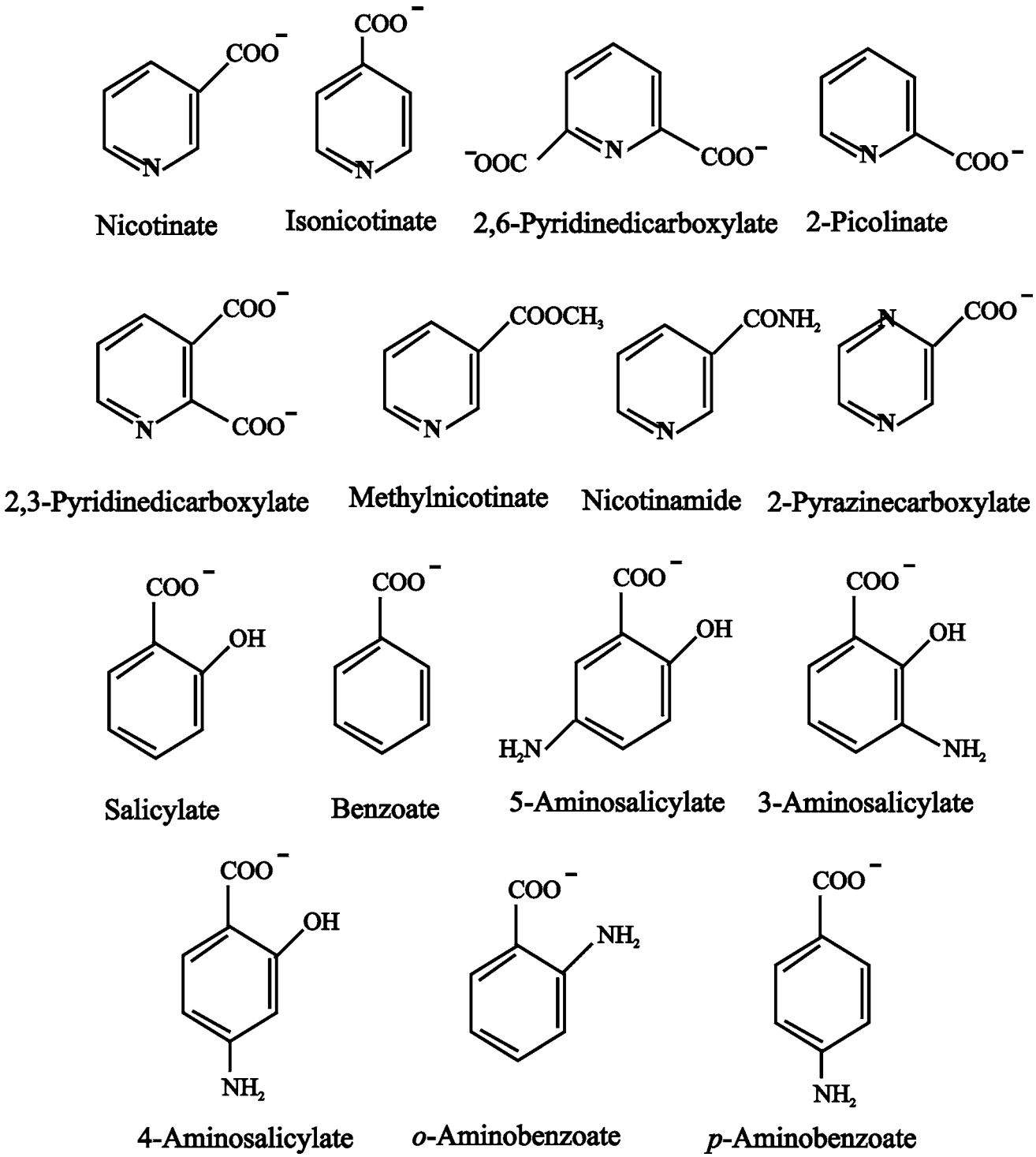

Fig. 1. Chemical structures of nicotinate and its structural analogs used in the present study.

robustly in *X. laevis* oocytes following injection with human SMCT1 cRNA. There was very little nicotinate uptake in control oocytes injected with water. In cRNA-injected oocytes, uptake of nicotinate (200 μM) was increased more than 80-fold compared to control oocytes. The induced uptake was entirely Na^+-dependent as the uptake was reduced to the levels found in control oocytes when measured in the absence of Na^+. Figure. 2b and c describe the effects of various monocarboxylates (2.5 mM), and structural analogs of nicotinate (5 mM) on the uptake of [^{14}C]nicotinate (100 μM) in SMCT1-expressing oocytes. SMCT1 is a transporter for lactate and pyruvate, and also

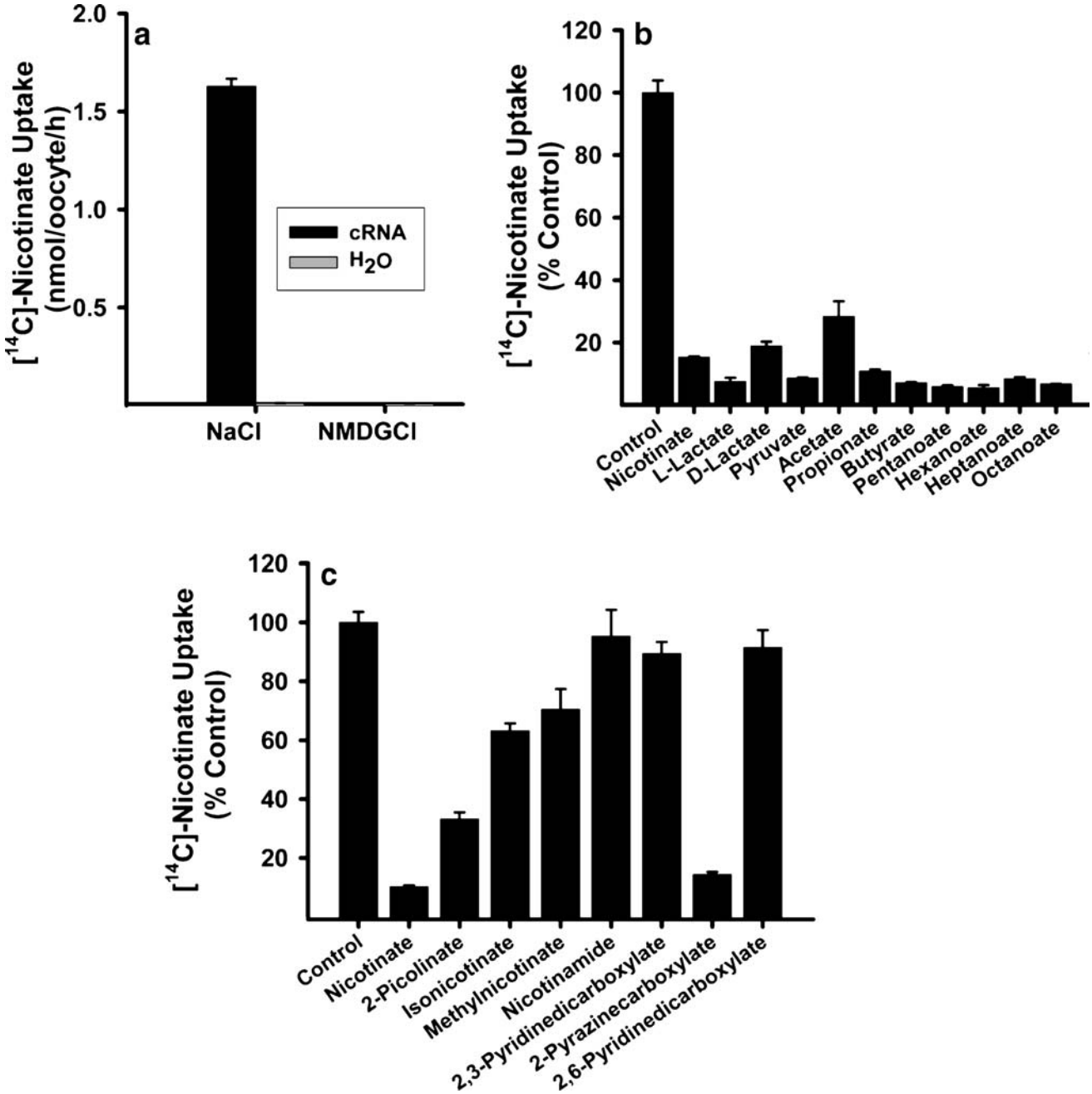

Fig. 2. Transport of nicotinate via human SMCT1 in *X. laevis* oocytes and its inhibition by short-chain/medium-chain fatty acids and by structural analogs of nicotinate. Human SMCT1 was expressed in oocytes by cRNA injection. Water-injected oocytes were used as control. **a** Uptake of [^{14}C]nicotinate (unlabeled plus radiolabeled nicotinate, 200 μM) was measured in cRNA-injected and water-injected oocytes for 60 min in the presence (NaCl) or absence (NMDG chloride) of Na^+. **b** Uptake of [^{14}C]nicotinate (unlabeled plus radiolabeled nicotinate, 100 μM) was measured in cRNA-injected oocytes for 60 min in the presence NaCl without (*control*) or with monocarboxylates (2.5 mM). **c** Uptake of [^{14}C]nicotinate (unlabeled plus radiolabeled nicotinate, 100 μM) was measured in cRNA-injected oocytes for 60 min in the presence NaCl without (*control*) or with structural analogs of nicotinate (5 mM). The uptake values in the presence of nicotinamide, 2,6-pyridinedicarboxylate, and 2,3-pyridinedicarboxylate are not statistically different from the control value, with p values 0.64, 0.22, and 0.07, respectively. The remaining uptake values are significantly less than the control value ($p < 0.05$).

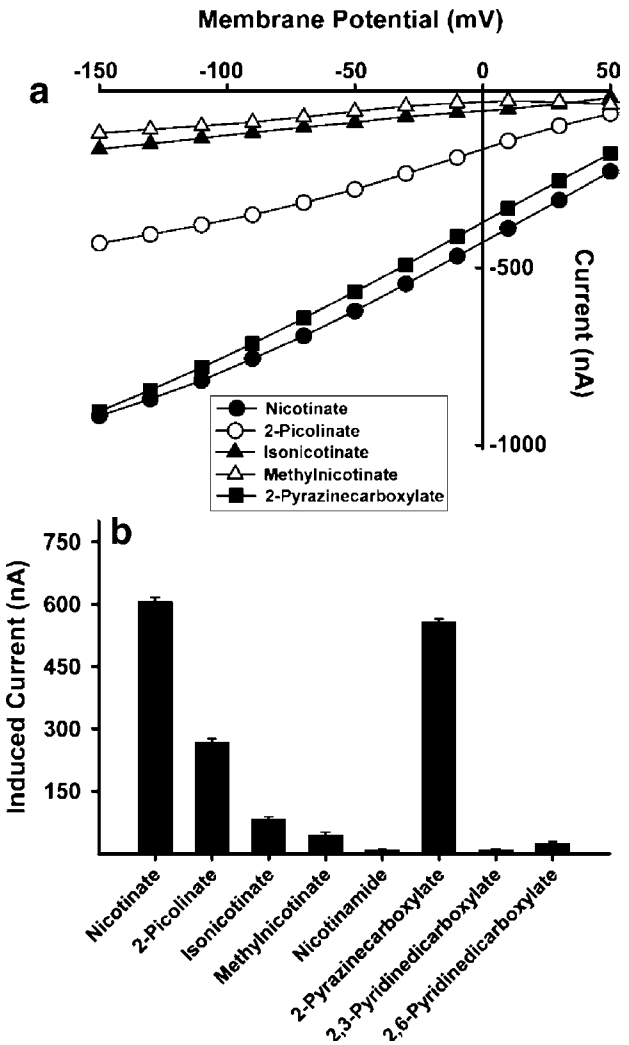

Fig. 3. Inward currents induced by nicotinate and its structural analogs via human SMCT1. Oocytes were perifused with a NaCl-containing buffer, followed by the same buffer containing nicotinate and its structural analogs. The differences between the steady-state currents measured in the presence and absence of substrates were considered as the substrate-induced currents. **a** Membrane potential–current (*I–V*) relationship for nicotinate and four of its structural analogs. **b** Magnitude of currents induced by nicotinate and its structural analogs at −50 mV.

for various short-chain and medium-chain fatty acids (1–3). Accordingly, SMCT1-mediated nicotinate uptake in oocytes was effectively inhibited by lactate, pyruvate, short-chain fatty acids (acetate, propionate, butyrate, and pentanoate) and medium-chain fatty acids (hexanoate, heptanoate, and octanoate). Among the nicotinate structural analogs examined, 2-picolinate and 2-pyrazinecarboxylate were the most potent inhibitors, followed by isonicotinate, and methylnicotinate. Nicotinamide, and nicotinate analogs containing two carboxylate groups did not have any effect.

The transport of nicotinate analogs via SMCT1 was monitored directly in SMCT1-expressing oocytes by studying inward currents induced by these compounds (5 mM) under voltage-clamp conditions (Fig. 3). Nicotinate, 2-pyrazinecarboxylate, 2-picolinate, isonicotinate, and methylnicotinate induced inward currents and the magnitude of the currents was influenced by membrane potential. Hyperpolarization of the membrane increased the magnitude of the currents whereas depolarization decreased the magnitude of the currents. There was a direct relationship between the potencies of these compounds to compete with [^{14}C]nicotinate for SMCT1-mediated uptake process (Fig. 2c) and the magnitude of the inward currents induced by these compounds (Fig. 3b). The more potent inhibitors induced more currents and the less potent inhibitors induced less currents, suggesting that the competition for interaction with the substrate-binding site of SMCT1 by these compounds is directly related to their transport. Nicotinamide and analogs with two carboxylate groups, which did not inhibit SMCT1-mediated [^{14}C]nicotinate uptake, did not induce significant currents,

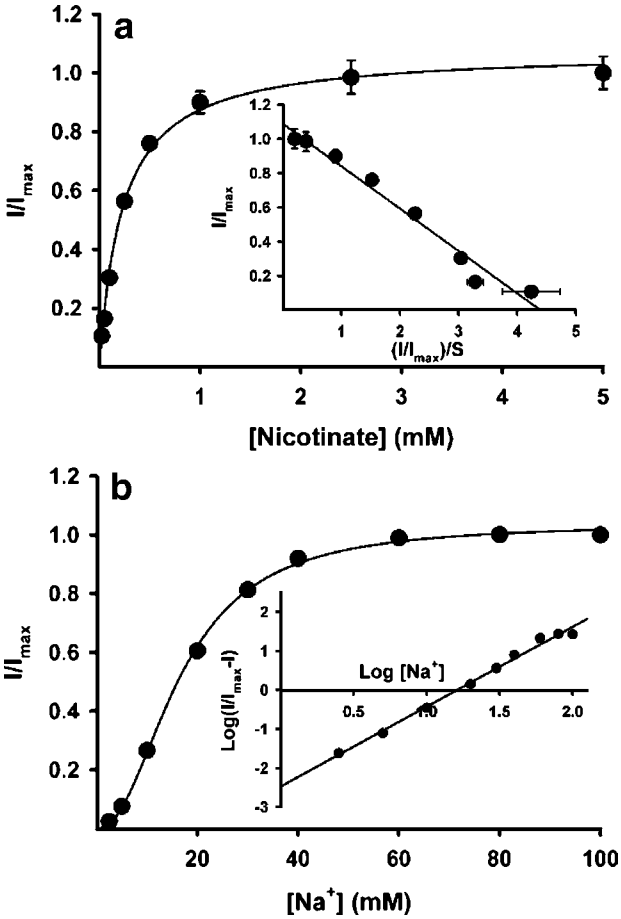

Fig. 4. Saturation kinetics and Na^+-activation kinetics for nicotinate-induced currents. **a** Inward currents induced by increasing concentrations of nicotinate were monitored at −50 mV in four different oocytes expressing human SMCT1. The data were normalized for variations in cRNA expression in different oocytes by taking the maximal value for the current induced by 5 mM nicotinate as 1 in each oocyte. *Inset*: Eadie–Hofstee plot. *Fitted lines* according to the non-linear or linear forms of the Michaelis–Menten equation are shown. **b** Inward currents induced by 5 mM nicotinate at increasing concentrations of Na^+ were monitored at −50 mV. The data were normalized for variations in cRNA expression in different oocytes by taking the maximal value for the current induced in the presence of 100 mM Na^+ as 1 in each oocyte. *Inset*: Hill plot. *Fitted lines* according to the non-linear or linear forms of the Hill equation are shown.

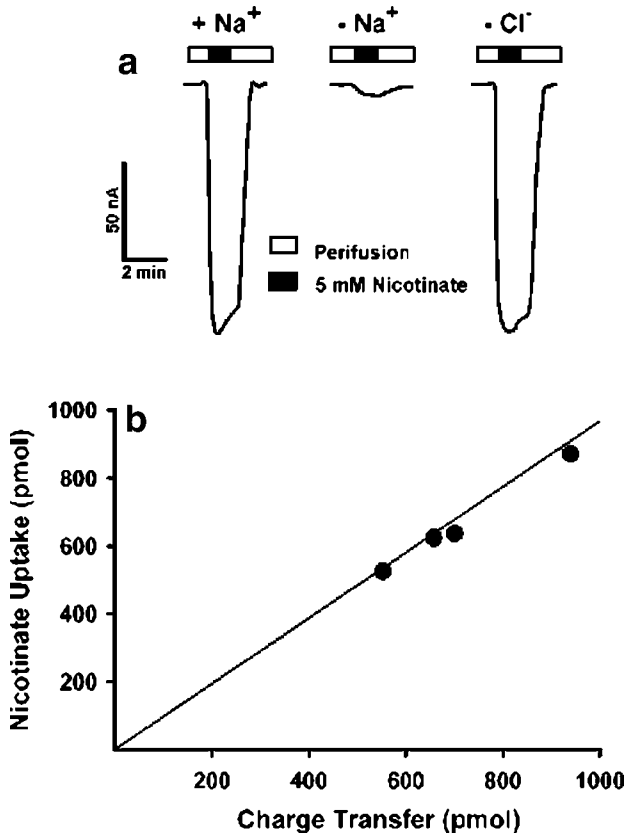

Fig. 5. Ion-dependence and substrate/charge transfer ratio for nicotinate transport mediated by human SMCT1 in oocytes. **a** Inward currents induced by nicotinate (5 mM) were monitored in oocytes expressing human SMCT1. Three different perifusion buffers were used which contain NaCl ($+Na^+$), NMDG chloride ($-Na^+$), or sodium gluconate ($-Cl^-$). **b** Oocytes expressing human SMCT1 were perifused with [^{14}C]nicotinate (unlabeled nicotinate, 85 μM; radiolabeled nicotinate, 15 μM) for 10 min and the inward currents induced by nicotinate were recorded. At the end of the perifusion, radioactivity associated with the oocytes was measured to determine the amount of nicotinate that has entered into the oocytes during the perifusion. The area *under* the current-time curve was integrated to calculate the amount of charge that has entered into the oocytes during the same period. Data are presented as the relationship between the amount of nicotinate transfer and the charge transfer.

indicating that these compounds are not recognized as substrates by the transporter.

Figure 4 describes the saturation kinetics and Na^+-activation kinetics for nicotinate transport via SMCT1 as monitored by nicotinate-induced currents. The transport was saturable and the data fit to the Michaelis–Menten equation describing a single saturable process. The Michaelis constant ($K_{0.5}$) for nicotinate was 230 ± 16 μM. The Na^+-activation of nicotinate-induced inward currents showed a sigmoidal pattern. Analysis of the data by the Hill equation yielded a value of 2.1 ± 0.1 for the Hill coefficient (h) and 17 ± 1 mM for $K_{0.5}$ for Na^+. These data suggest a Na^+:nicotinate stoichiometry of 2:1 for the transport process. This was confirmed by direct determination of the substrate/charge transfer ratio. The inward currents induced by nicotinate (5 mM) in SMCT1-expressing oocytes were obligatorily dependent on the presence of Na^+ (Fig. 5a). There was no involvement of Cl^- in the process. This indicates that currents induced by nicotinate are entirely due to cotransport of Na^+ and nicotinate. The substrate/charge transfer ratio, determined in four different oocytes, was 0.95 ± 0.01 (Fig. 5b), indicating that one positive charge was transferred into oocyte along with every molecule of nicotinate transported via SMCT1. Nicotinate exists as a monovalent anion under the experimental conditions and therefore the substrate/charge transfer ratio of close to 1 corroborates with the data from the Na^+-activation kinetics which gave a value of 2:1 for Na^+:nicotinate stoichiometry.

Transport of Monocarboxylate Drugs Via Human SMCT1

We examined the interaction of several monocarboxylates with human SMCT1. Initially, we determined the

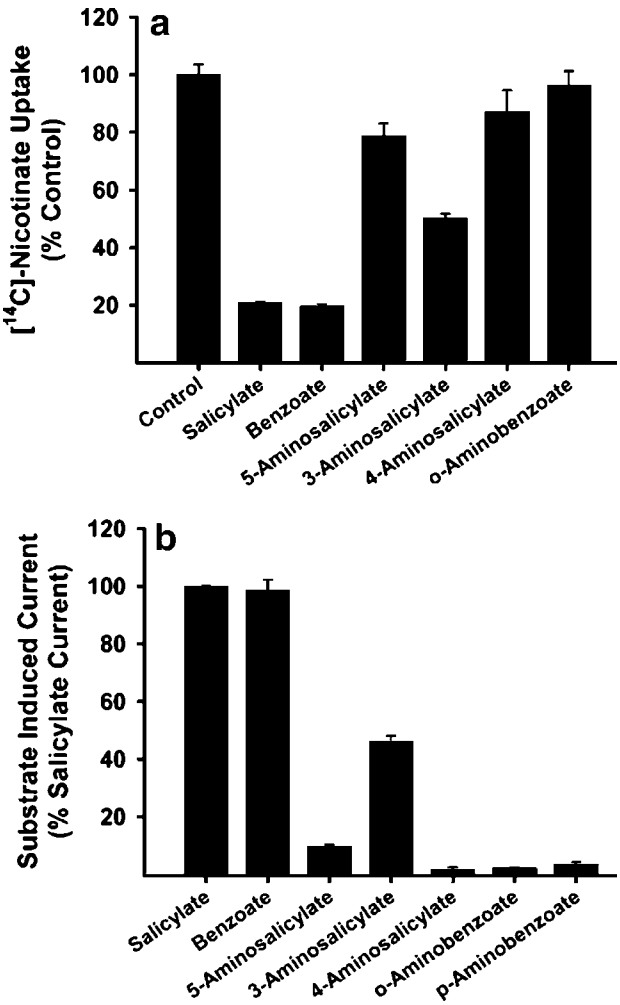

Fig. 6. Transport of monocarboxylate drugs via human SMCT1. **a** Uptake of [^{14}C]nicotinate (unlabeled plus radiolabeled nicotinate, 100 μM) was measured in oocytes expressing human SMCT1 in a Na^+-containing buffer in the absence (*control*) or presence of various monocarboxylate drugs (5 mM). **b** Inward currents induced by various monocarboxylate drugs (5 mM) were monitored at −50 mV in a Na^+-containing buffer in oocytes expressing human SMCT1. The uptake values in the presence of *o*-aminobenzoate and 4-aminosalicylate are not statistically different from the control value, with p values 0.56 and 0.13, respectively. The remaining uptake values are significantly less than the control value ($p < 0.05$).

ability of these compounds (5 mM) to compete with [^{14}C]nicotinate (100 μM) for the uptake process (Fig. 6a). Benzoate, salicylate, 3-aminosalicylate, and 5-aminosalicylate were able to inhibit nicotinate uptake to a significant extent, with the following order of potency: benzoate = salicylate > 3-aminosalicylate > 5-aminosalicylate. 4-Aminosalicylate, *o*-aminobenzoate, and *p*-aminobenzoate showed little or no effect. This corroborated with the magnitude of the inward currents induced by these compounds (5 mM) under voltage-clamp conditions (Fig. 6b). Benzoate and salicylate induced the maximum currents, followed by 3-aminosalicylate and then by 5-aminosalicylate. The compounds, which had no effect on nicotinate uptake, showed negligible currents. Figure 7 describes the saturation kinetics for benzoate and salicylate. The currents induced by both compounds were saturable, following the Michaelis–Menten equation describing a single saturable transport system. The $K_{0.5}$ was 1.1 ± 0.2 mM for benzoate and 1.5 ± 0.1 mM for salicylate. Figure 8 describes the saturation kinetics and Na^+-activation kinetics for 5-aminosalicylate. The transport of 5-aminosalicylate via

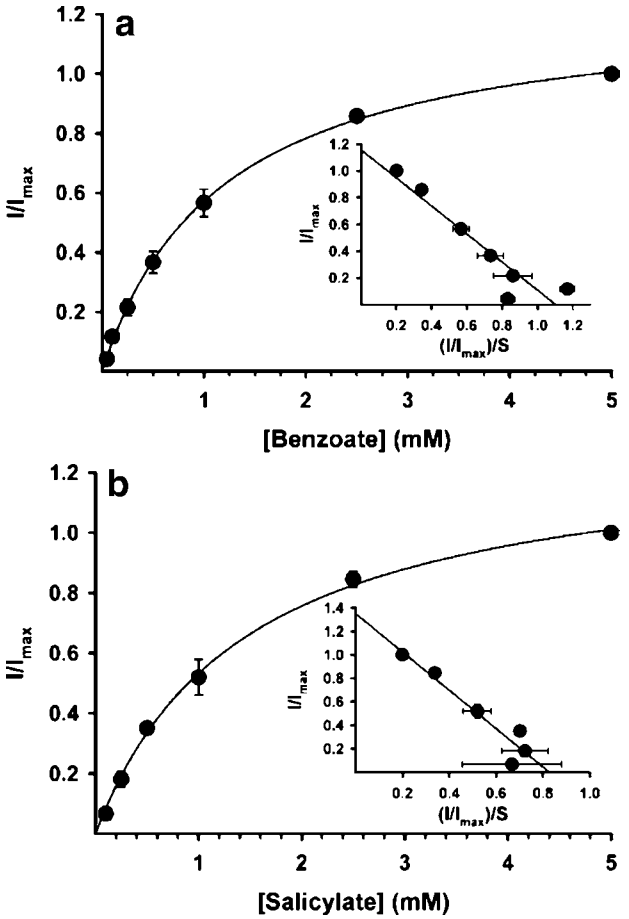

Fig. 7. Saturation kinetics for benzoate **a** and salicylate **b** for transport via human SMCT1. Inward currents induced by increasing concentrations of benzoate or salicylate were monitored at −50 mV in a Na^+-containing buffer in oocytes expressing human SMCT1. The data were normalized for variations in cRNA expression in different oocytes by taking the maximal value for the current induced 5 mM benzoate or salicylate as 1 in each oocyte. *Insets*: Eadie–Hofstee plot. *Fitted lines* according to the non-linear or linear forms of the Michaelis–Menten equation are shown.

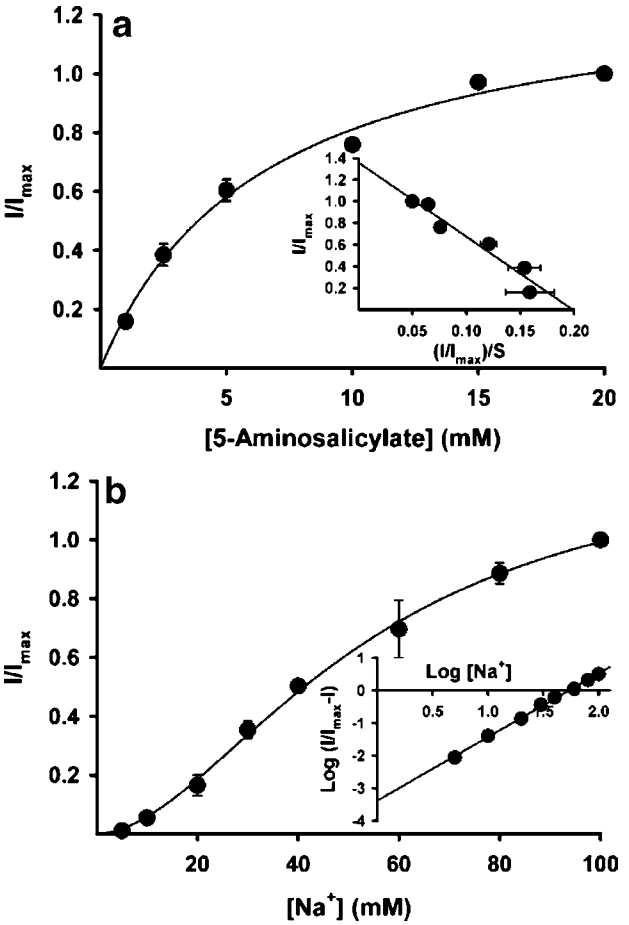

Fig. 8. Saturation kinetics and Na^+-activation kinetics for currents induced by 5-aminosalicylate. **a** Inward currents induced by increasing concentrations of 5-aminosalicylate were monitored at −50 mV in four different oocytes expressing human SMCT1. The data were normalized for variations in cRNA expression in different oocytes by taking the maximal value for the current induced by 20 mM 5-aminosalicylate as 1 in each oocyte. *Inset*: Eadie–Hofstee plot. *Fitted lines* according to the non-linear or linear forms of the Michaelis–Menten equation are shown. **b** Inward currents induced by 10 mM 5-aminosalicylate at increasing concentrations of Na^+ were monitored at −50 mV. The data were normalized for variations in cRNA expression in different oocytes by taking the maximal value for the current induced in the presence of 100 mM Na^+ as 1 in each oocyte. *Inset*: Hill plot. *Fitted lines* according to the non-linear or linear forms of the Hill equation are shown.

SMCT1 was saturable with a $K_{0.5}$ of 6.5 ± 1.0 mM (Fig. 8a). Na^+-activation of the transport process showed sigmoidal kinetics with a Hill coefficient of 2.0 ± 0.1 and a $K_{0.5}$ of 54 ± 6 mM.

EXPRESSION PATTERN AND POLARIZED LOCALIZATION OF SMCT1 IN THE MAMMALIAN INTESTINAL TRACT

We examined the expression of SMCT1 along the mouse intestinal tract by immunofluorescence using an antibody specific for SMCT1. The transporter was expressed in the jejunum (Fig. 9a), ileum (Fig. 9b), as well as colon (Fig. 9c). In all cases, the expression was restricted to the lumen-facing

apical membrane of the intestinal/colonic epithelial cells. The antibody that had been neutralized with the antigenic peptide did not give any detectable positive signal under identical conditions (Fig. 9d). We also examined the expression of the transporter in human colon (Fig. 9e). The expression was clearly evident in the apical membrane of the colonic epithelial cells. It was interesting that the expression was not uniform in all cells lining the surface of the human colon, but we suspect that this is due to the fact that the sections used in these studies were from archival tissue rather than

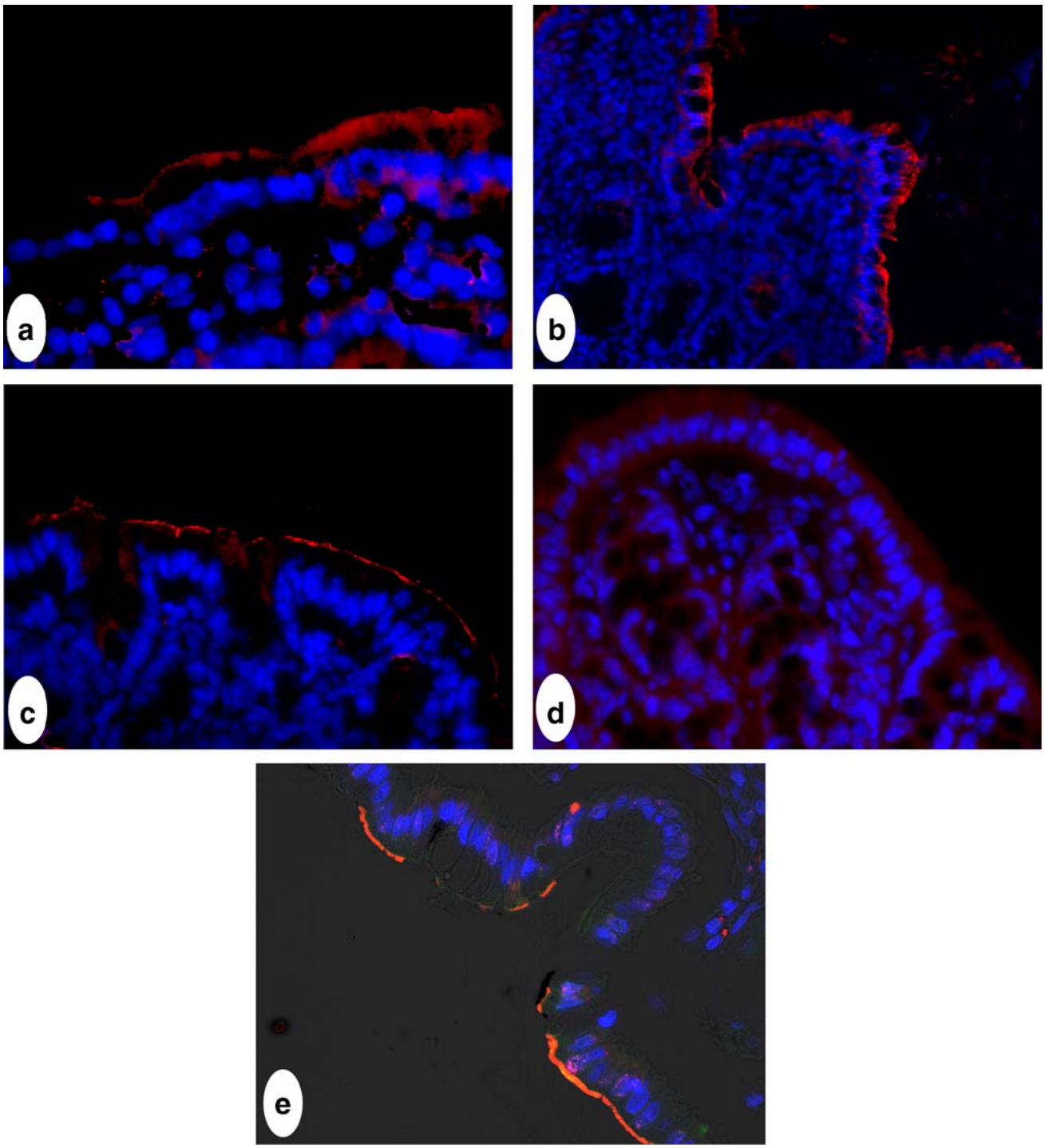

Fig. 9. Immunofluorescence localization of SMCT1 in intestinal tract. Sections of mouse jejunum, ileum, and colon, and human colon were incubated first with an antibody specific for SMCT1 (rabbit polyclonal), and then with a secondary antibody (goat anti-rabbit IgG)-conjugated with a red fluorophore. DAPI (*blue fluorescence*) was used as a nuclear stain. For negative control, sections of mouse colon were incubated first with the SMCT1 antibody that had been neutralized with the antigenic peptide and then processed in an identical manner as described above. **a**, mouse jejunum; **b**, mouse ileum; **c**, mouse colon; **d**, negative control with mouse colon; **e** human colon.

from fresh samples. When fresh tissue was used as was done with mouse jejunum, ileum, and colon, the expression of the transporter was uniform in all cells.

DISCUSSION

Recently we reported on the identity of the transport function of human SLC5A8 and mouse slc5a8 (1,3). These transporters mediate Na^+-coupled transport of short-chain fatty acids as well as the monocarboxylates lactate and pyruvate. Accordingly, this transporter was named SMCT1 (Sodium-coupled MonoCarboxylate Transporter 1). The B-complex vitamin nicotinate is also a monocarboxylate and its absorption in the kidney proximal tubule is known to occur via a Na^+-coupled mechanism (17). Since SMCT1 is expressed in the intestinal tract and kidney, we asked if this transporter is responsible for nicotinate absorption. Subsequent studies in our laboratory showed that mouse SMCT1 is indeed capable of transporting nicotinate in a Na^+-coupled manner (13). The $K_{0.5}$ value for nicotinate is in the range of 170–300 μM depending on the expression system used, and the Na^+:nicotinate stoichiometry is 2:1. The transporter also recognizes several structural analogs of nicotinate as substrates. We initiated the present studies for three reasons. First, we wanted to investigate the handling of nicotinate and its structural analogs by human SMCT1 and compare the kinetic features and substrate specificity of this transporter with those of mouse SMCT1. There are instances where the mouse and human orthologs differ markedly in transport characteristics. For example, mouse and rat NaCT, a Na^+-coupled citrate transporter, show a $K_{0.5}$ of ~20 μM for citrate (16,18) whereas the corresponding value for human NaCT is ~650 μM (19). The transport function of mouse and rat NaCT is inhibited by Li^+ whereas the transport function of human NaCT is stimulated by Li^+ (20). Therefore, we felt that it was essential to characterize the handling of nicotinate and its structural analogs by human SMCT1. Second, though human and mouse SMCT1 transport monocarboxylates in an electrogenic manner, the charge/substrate transfer ratio seems to vary depending on the substrate. With lactate as the substrate, the ratio is 1, but the value is 2 for propionate (1,3). The substrate/charge transfer ratio has not yet been reported for nicotinate. Therefore, we wanted to determine this value for human SMCT1. Third, though we have already reported on the handling of various structural analogs of nicotinate by mouse SMCT1, little is known at present on the ability of SMCT1 to transport monocarboxylate drugs. Therefore, we wanted to examine the interaction of several monocarboxylate drugs with this transporter.

The results of the present study can be summarized as follows. Similar to mouse SMCT1, human SMCT1 also interacts with nicotinate and several of its structural analogs and transports them in a Na^+-coupled manner. The $K_{0.5}$ for nicotinate (230 μM) and the Na^+:nicotinate stoichiometry (2:1) are similar to those for the mouse ortholog. The substrate/charge transfer ratio for nicotinate is 1, suggesting cotransport of 2 Na^+ per nicotinate. This value is similar to that for lactate but differs from the value reported for propionate.

The present study also focused for the first time on the ability of SMCT1 to handle monocarboxylate drugs. We found that salicylate and benzoate are recognized as transportable substrates by human SMCT1 with appreciable affinity ($K_{0.5}$, ~1 mM). In addition, we found that 3-aminosalicylate and 5-aminosalicylate also serve as substrates for the transporter, but the affinity is lower than that for benzoate or salicylate. Though the transport of both nicotinate and 5-aminosalicylate exhibits sigmoidal Na^+-activation kinetics with a Na^+:substrate stoichiometry of 2:1, one clear difference between the two substrates was noticeable. With nicotinate as the substrate, activation of transport saturates at a Na^+ concentration of ~60 mM with a $K_{0.5}$ value of 17 ± 1 mM. In contrast, the transport of 5-aminosalicylate does not saturate even at a Na^+ concentration of 100 mM. The $K_{0.5}$ for Na^+ to activate the transport of 5-aminosalicylate is three-fold higher than that for nicotinate as the substrate (54 ± 6 mM versus 17 ± 1 mM). These data suggest that molecular structure and/or size of the substrate may influence the interaction of Na^+ with the transporter. This does not necessarily give any information on whether Na^+ binds first followed by the substrate or the substrate binds first followed by Na^+. But, it shows that the substrate-binding site and the Na^+-binding site should be spatially related, the conformation of one influencing the conformation of the other. The $K_{0.5}$ for Na^+ has been shown to change in response to varying substrate concentrations or membrane potential in the case of other members of the *SLC5* gene family. For example, the $K_{0.5}$ for Na^+ decreases with increasing membrane potential for the Na^+-coupled glucose transporter SGLT1 (21), and with increasing substrate concentration for the Na^+-coupled iodide transporter NIS (22). However, there is no information available in the literature for any member of this gene family on the influence of different substrates with varying affinity on the $K_{0.5}$ for Na^+. Further studies are needed to define this interesting feature observed with SMCT1 in more detail.

In order to understand the scope of SMCT1 as a transporter for monocarboxylate drugs in the intestinal tract, we determined its expression pattern along the mouse intestinal tract and also its polarized expression in enterocytes/colonocytes. The transporter is expressed in the jejunum, ileum, and colon in the mouse where its expression is restricted to the lumen-facing apical membrane. We were also able to demonstrate the expression of the transporter in the apical membrane of colonocytes in human colon. This suggests that the transporter may contribute to the intestinal/colonic absorption of monocarboxylate drugs. In this respect, the handling of salicylates by the transporter is particularly relevant. 5-Aminosalicylate represents the drug of choice for the treatment of ulcerative colitis (23,24). The drug is administered either in the form of azo-prodrugs (sulfasalazine, olsalazine or balsalazide) or in its free form. The ultimate therapeutic target site for these drugs is the colon. Upon reaching the colon, 5-aminosalicylate is released from the azo-prodrugs by bacterial action. When administered orally in its free form, it is formulated in such a manner that the drug reaches the colon. These drugs are also taken as rectal suppositories or enema to maximize their delivery to the colon. The therapeutic actions of 5-aminosalicylate are local, acting on the inflamed colonic mucosal cells. 5-Aminosalicylate is an inhibitor of cyclooxygenases and lipoxygenases, an effective scavenger of free radicals, and also an inhibitor of NF-κB activation (25,26). Therefore, the drug has

to enter the inflamed colon cells to produce these effects; but how this monocarboxylate drug enters the cells is not known. Present studies demonstrating the expression of SMCT1 in the colonic apical membrane and the transport of 5-aminosalicylate via the transporter suggest that the entry of the drug into colonocytes may be at least partly mediated by this transporter. The expression of the transporter in the apical membrane of the enterocytes in the small intestine indicates that SMCT1 may also play a significant role in the oral absorption of other monocarboxylate drugs. Several studies have implicated the H^+-coupled monocarboxylate transporter MCT1 in the intestinal absorption of monocarboxylate drugs (27). SMCT1 may complement MCT1 in this process.

REFERENCES

1. S. Miyauchi, E. Gopal, Y. J. Fei, and V. Ganapathy. Functional identification of SLC5A8, a tumor suppressor down-regulated in colon cancer, as a Na^+-coupled transporter for short-chain fatty acids. *J. Biol. Chem* **279**:13293–13296 (2004).
2. M. J. Coady, M. H. Chang, F. M. Charron, C. Plata, B. Wallendorff, J. F. Sah, S. D. Markowitz, M. F. Romero, and J. Y. Lapointe. The human tumour suppressor gene SLC5A8 expresses a Na^+-monocarboxylate cotransporter. *J. Physiol.* **557**:719–731 (2004).
3. E. Gopal, Y. J. Fei, M. Sugawara, S. Miyauchi, L. Zhuang, P. M. Martin, S. B. Smith, P. D. Prasad, and V. Ganapathy. Expression of slc5a8 in kidney and its role in Na^+-coupled transport of lactate. *J. Biol. Chem.* **279**:44522–44532 (2004).
4. H. Li, L. Myeroff, D. Smiraglia, M. F. Romero, T. P. Pretlow, L. Kasturi, J. Lutterbaugh, R. M. Rerko, G. Casey, J. P. Issa, J. Willis, J. K. Willson, C. Plass, and S. D. Markowitz. SLC5A8, a sodium transporter, is a tumor suppressor gene silenced by methylation in human colon aberrant crypt foci and cancers. *Proc. Natl. Acad. Sci. U. S. A.* **100**:8412–8417 (2003).
5. V. Ganapathy, E. Gopal, S. Miyauchi, and P. D. Prasad. Biological functions of SLC5A8, a candidate tumour suppressor. *Biochem. Soc. Trans.* **33**:237–240 (2005).
6. N. Gupta, P. M. Martin, P. D. Prasad, and V. Ganapathy. SLC5A8 (SMCT1)-mediated transport of butyrate forms the basis for the tumor suppressive function of the transporter. *Life Sci.* **78**:2419–2425 (2006).
7. M. Thangaraju, S. Ananth, P. M. Martin, P. Roon, S. B. Smith, E. Sterneck, P. D. Prasad, and V. Ganapathy. c/ebpd null mouse as a model for the double-knockout of slc5a8 and slc5a12 in kidney. *J. Biol. Chem*. **281**:26769–26773 (2006).
8. P. M. Martin, E. Gopal, S. Ananth, L. Zuang, S. Itagaki, B. M. Prasad, S. B. Smith, P. D. Prasad, and V. Ganapathy. Identity of SMCT1 (SLC5A8) as a neuron-specific Na^+-coupled transporter for active uptake of L-lactate and ketone bodies in the brain. *J. Neurochem.* **98**:279–288 (2006).
9. R. L. Veech, B. Chance, Y. Kashiwaya, H. A. Lardy, and G. F. Cahill Jr. Ketone bodies, potential therapeutic uses. *IUBMB Life* **51**:241–247 (2001).
10. K. Casteels and C. Mathieu. Diabetic ketoacidosis. *Rev. Endocr. Metab. Disord.* **4**:159–166 (2003).
11. A. M. Rodriguez, B. Perron, L. Lacroix, B. Caillou, G. Leblanc, M. Schlumberger, J. M. Bidart, and T. Pourcher. Identification and characterization of a putative human iodide transporter located at the apical membrane of thyrocytes. *J. Clin. Endocrinol. Metab.* **87**:3500–3503 (2002).
12. V. Paroder, S. R. Spencer, M. Paroder, D. Arango, S. Schwartz Jr., J. M. Mariadason, L. H. Augenlicht, S. Eskandari, and N. Carrasco. Na^+/monocarboxylate transport (SMCT) protein expression correlates with survival in colon cancer: molecular characterization of SMCT. *Proc. Natl. Acad. Sci. USA* **103**:7270–7275 (2006).
13. E. Gopal, Y. J. Fei, S. Miyauchi, L. Zhuang, P. D. Prasad, and V. Ganapathy. Sodium-coupled and electrogenic transport of B-complex vitamin nicotinic acid by slc5a8, a member of the Na/glucose co-transporter gene family. *Biochem. J.* **388**:309–316 (2005).
14. S. Itagaki, E. Gopal, L. Zuang, Y. J. Fei, S. Miyauchi, P. D. Prasad, and V. Ganapathy. Interaction of ibuprofen and other structurally related NSAIDs with the sodium-coupled monocarboxylate transporter SMCT1 (SLC5A8). *Pharm. Res.* **23**:1209–1216 (2006).
15. H. Wang, Y. J. Fei, R. Kekuda, T. L. Yang-Feng, L. D. Devoe, F. H. Leibach, P. D. Prasad, and V. Ganapathy. Structure, function, and genomic organization of human Na^+-dependent high-affinity dicarboxylate transporter. *Am. J. Physiol.* **278**: C1019–C1030 (2000).
16. K. Inoue, Y. J. Fei, L. Zhuang, E. Gopal, S. Miyauchi, and V. Ganapathy. Functional features and genomic organization of mouse NaCT, a sodium-coupled transporter for tricarboxylic acid cycle intermediates. *Biochem. J.* **378**:949–957 (2004).
17. S. Schuette and R. C. Rose. Renal transport and metabolism of nicotinic acid. *Am. J. Physiol.* **250**:C694–C703 (1986).
18. K. Inoue, L. Zhuang, D. M. Maddox, S. B. Smith, and V. Ganapathy. Structure, function, and expression pattern of a novel sodium-coupled citrate transporter (NaCT) cloned from mammalian brain. *J. Biol. Chem.* **277**:39469–39476 (2002).
19. K. Inoue, L. Zhuang, and V. Ganapathy. Human Na^+-coupled citrate transporter (NaCT): primary structure, genomic organization, and transport function. *Biochem. Biophys. Res. Commun.* **299**:465–471 (2002).
20. K. Inoue, L. Zhuang, D. M. Maddox, S. B. Smith, and V. Ganapathy. Human NaCT, the ortholog of Drosophila Indy, as a novel target for lithium action. *Biochem. J.* **374**:21–26 (2003).
21. M. Panayatova-Heiermann, D. D. Loo, and E. M. Wright. Kinetics of steady-state currents and charge movements associated with the rat Na^+/glucose cotransporter. *J. Biol. Chem.* **270**:27099–27105 (1995).
22. S. Eskandari, D. D. Loo, G. Dai, O. Levy, E. M. Wright, and N. Carrasco. Thyroid Na^+/I^- symporter. Mechanism, stoichiometry, and specificity. *J. Biol. Chem.* **272**:27230–27238 (1997).
23. M. D. Regueiro. Diagnosis and treatment of ulcerative colitis. *J. Clin. Gastroenterol.* **38**:733–740 (2004).
24. C. T. Xu, S. Y. Meng, and B. R. Pan. Drug therapy for ulcerative colitis. *World J. Gastroenterol.* **10**:2311–2317 (2004).
25. R. P. MacDermott. Progress in understanding the mechanisms of action of 5-aminosalicylic acid. *Am. J. Gastroenterol.* **95**: 3343–3345 (2000).
26. J. P. Gisbert, F. Gomollon, J. Mate, and J. M. Pajares. Role of 5-aminosalicylic acid (5-ASA) in treatment of inflammatory bowel disease: a systematic review. *Dig. Dis. Sci.* **47**:471–488 (2002).
27. B. E. Enerson and L. R. Drewes. Molecular features, regulation, and function of monocarboxylate transporters: Implications for drug delivery. *J. Pharm. Sci.* **92**:1531–1544 (2003).